Turkish Journal of Engineering

https://dergipark.org.tr/en/pub/tuje

e-ISSN 2587-1366

Wear Studies on Nano Silicon Carbide Particle Strengthened AZ31 Magnesium Nano Surface Composites Developed via Friction Stir Processing

N. Senthilkumar[1], B. Deepanraj*[2], Feroz Shaik[2], V. Nadanakumar[3]

[1] Saveetha School of Engineering, Saveetha Institute of Medical and Technical Sciences, Chennai, 602105, India, nskmfg@gmail.com
[2] Department of Mechanical Engineering, College of Engineering, Prince Mohammad Bin Fahd University, Al Khobar, 31952, Saudi Arabia, babudeepan@gmail.com, ferozs2005@gmail.com
[3] Department of Automobile Engineering, Hindustan Institute of Technology and Science, Chennai, 306103, India, vin.nadanakumar@gmail.com

Cite this study: Senthilkumar, N., Deepanraj, B., Shaik, F. & Nadanakumar, V. (2025). Wear Studies on Nano Silicon Carbide Particle Strengthened AZ31 Magnesium Nano Surface Composites Developed via Friction Stir Processing. Turkish Journal of Engineering, 9 (3), 425-432.

https://doi.org/10.31127/tuje.1531603

Keywords
AZ31
Nano silicon carbide
Friction stir processing
Pin-on-disc
Wear rate

Research/Review Article

Received:13.08.2024
Revised:02.09.2024
Accepted:16.09.2024
Published:01.07.2025

Abstract

This article evaluates the impact of nano silicon carbide (nSiC) addition (0, 1, 2, 3, and 4 wt.%) on the surface of AZ31 magnesium alloy towards improvement in wear resistance for different applied load (AL) and sliding distance (SD). Friction stir processing (FSP) is performed on the surface of AZ31 to create a weld pool to disperse the nSiC particles utilizing a cylindrical tool in a computerized controlled machine tool. The study objective is to enhance the wear resilience of the lightweight soft AZ31 through this procedure. The G99 standard of ASTM was adopted for performing the experimentations. nSiC added to the surface lowers the wear rate (WR) of the FSPed specimens subjected to different AL and SD. The coefficient of friction (CoF) and WR tend to drop with the inclusion of nSiC till 3 wt.% above which a negative trend is observed due to the improper bonding and agglomeration of nSiC particles that impart lesser strength and hardness on the surface. As compared with an AL of 10 N, the AL of 50 N produces a 171.43% higher WR for as received alloy, for AZ31+3%nSiC, the WL is increased by 337.5% whereas the CoF is increased by 14.93% for as received alloy and 15.15% for AZ31+3%nSiC composite. Similarly, increasing the SD from 250 to 1250m, the WR is doubled for as received alloy and 181.82% for AZ31+3%nSiC, the CoF is increased by 0.41%.

1. Introduction

Surface modification (SM) is a common way to improve a substrate's surface characteristics. SM techniques can help lightweight alloys meet their specific needs in various applications. Light alloys are used in many industries, including the military, automotive, aerospace, sports, electronics, and biomedical sectors [1]. SM techniques can improve surface properties like wear and corrosion resistance, inhibit oxidation, promote adhesion of further coatings, construct an anti-corrosion layer with good surface biocompatibility, and enhance mechanical integrity, biodegradation, and biocompatibility [2-4]. Magnesium and its alloys are susceptible to corrosion and wear under harsh environments; hence, surface treatments or modifications are needed to improve its performance without altering its core properties [5].

The techniques used for surface coatings include chemical conversion coating, electrodeposition, laser surface modification, calcium phosphate surface coatings, plasma electrolytic oxidation, and magnetron sputtering [6]. Friction stir processing (FSP) is a procedure used for solid-state welding and surface engineering. It can enhance various properties of metals, such as formability, durability to corrosion, elasticity, strength, hardness, and resistance to abrasion [7]. FSP has the potential to enhance various properties, including eliminating casting defects, refining microstructures, improving strength and ductility, increasing resistance to corrosion and fatigue, and enhancing formability. The FSP process ensures a

consistent distribution of reinforcement particles, eliminating porosity and preventing undesired interfacial reactions between the matrix and the particles. FSP produce a fine-grained microstructure in the processed zone, which significantly improves mechanical properties such as strength, hardness, and wear resistance. Unlike traditional methods that may involve high temperatures or chemicals, FSP is a solid-state process, which does not melt the material, thereby avoiding porosity, cracking, or thermal distortion. Additionally, FSP is highly controllable and localized, allowing for precise modification of specific areas without affecting the entire component. Moreover, FSP is environmentally friendly, as it requires no harmful chemicals or extensive post-processing [8].

Subramani et al. [9] prepared AZ31 composites reinforced with nano silicon carbide (nSiC) particles using a stir casting procedure. The microstructure investigation exposed the presence of discontinuous Mg17Al12 phases and a well-distributed population of nSiC nanoparticles. The fabricated nanocomposites exhibited improvements in hardness and yield strength. The mechanical possessions and wear resistance progressively improved as the nSiC content in the nanocomposite increased. The wear behavior of the fabricated nanocomposites exhibited an inverse relationship with their hardness. In their study, Shen et al. [10] examined the tribological features of SiCp-reinforced Mg composite under various loads and sliding velocities. The addition of SiCp effectively inhibits grain evolution and enhances the composite's mechanical properties. As the sliding speed or load increases, the composite's wear rate (WR) gradually rises. When compared to the alloy, there is a significant reduction in the wear, specifically under high load conditions. Padmavathi et al. [11] examined the effects of BN and SiC blending ratios, interfacial activities, metallography, and mechanical properties of an AZ31 composite. The squeeze stir cast method was used to produce the composite. The composite exhibits a homogenous distribution of particles, with a composition of 5wt% BN and 7.5wt%. The material SiC demonstrated superior tensile strength, optimal strain, improved impact resistance, and increased hardness. Abdollahzadeh et al. [12] investigated the AZ31-nSiC composite mechanical and microstructural characteristics. The findings suggest that the size of the matrix grain and nSiC play crucial roles in determining various characteristics. Adjusting rotation and traverse speed leads to significant heat generation and uniform dispersion of nSiC.

Kumar et al. [13] investigated the wear characteristics of composites fortified with 15 vol.% Zirconium dioxide (ZrO_2) in AZ31 matrix. The enhancement in both hardness and tensile strength was ascribed to the grain size reduction, leading to Orowan strengthening. A clear relationship was observed between the WR and speed, characterized by an initial rise and subsequent decline. It is clear from the micrographs that the particular WR increases as the particles are higher. Abrasion is also the main process that removes materials. Kumar et al. [14] examined a surface composite's dry sliding wear properties with FSPed AZ31 and AZ31/ZrC particles dispersed throughout at 5, 10, and 15 vol.%. Abrasion, delamination, oxidation, material softening, and plastic deformation are the primary wear processes. The wear resistance of AZ31 alloy was observed to greatly enhance with an increased volume of ZrC, irrespective of the speed and load conditions.

In their study, Xiong et al. [15] performed laser alloying of SiC-316L powder on the AZ31 surface. The results suggest that the surface of the alloying layer was smooth and well-bonded, showing no signs of defects like pilling, pores, or cracks. The alloying layer comprises elements such as MgO and SiO_2 and the initial phases of Fe, SiC, and Mg. The grain boundary faces the alloyed layer and runs perpendicular to the interface. The magnesium alloy substrate lies at its base, where the alloyed layer and interface zone are located. In their study, Jiang et al. [16] employed the gas tungsten arc technique to apply SiC particles onto the AZ31 alloy substrate. Grain size inside the composite layer was significantly reduced due to the method. The composite layer establishes enhanced hardness and wear resistance compared to the original magnesium alloy AZ31. The material's properties are affected by various factors, including the process parameters and the concentration and distribution of SiC particles. Arora et al. [17] utilized FSP to develop a nanocomposite using AZ31 as the base material and TiC as the reinforcing agent. The experiments were conducted under various cooling conditions. The study found that the examined Mg alloy underwent substantial wear due to abrasion, delamination, and oxidation.

The literature survey presents that SM technique can be utilized effectively to modify the surface of the lightweight alloy without changes in the core properties. Magnesium alloys are preferably used in FSP to improve its wear and corrosion resistance. Including nanoparticles is done in lower quantities to make it more economical and avoid accumulation. This work deals with the FSP of AZ31 alloy incorporated with nSiC particles in varying proportions to achieve better dispersal and wear durability and subsequent wear analysis on the surface, which is the novelty of the present study. An analysis was conducted on the WR and CoF of the FSPed specimens. The wear tests involved varying the axial load (AL) and sliding distance (SD). The objective was to determine the optimal proportion of nSiC on the surface of AZ31.

2. Method

AZ31 is a frequently utilized magnesium alloy in various non-automotive applications. This magnesium alloy is highly favored for its lightweight behaviour and impressive mechanical qualities. The AZ31 consists of 3% aluminum, 1% zinc, and 0.5% manganese; the remaining balance is magnesium [18]. AZ31 is a magnesium alloy known for its favorable strength and flexibility at room temperature. In addition, it possesses excellent corrosion resistance and can be easily welded. It is a viable substitute for aluminum alloys because of its remarkable strength-to-weight proportion, lightweight nature, and superior machinability [19]. Nano silicon carbide (nSiC) is a semiconductor material known for its

high-temperature oxidation resistance. The material exhibits excellent thermal conductivity, stability, purity, and wear resistance. The use of nanoparticles extends to high-temperature spray nozzles and sealing valves [20]. nSiC surface-modified magnesium alloys have significant potential in various high-performance applications like aircraft frames and engine components, more durable and lightweight engine blocks, transmission cases, and other critical parts, contributing to fuel efficiency and performance. Additionally, in biomedical applications, ideal for use in biodegradable implants and medical devices, and heat sinks in electronics. The AZ31 alloy is purchased from M/s. Bhandari metals and alloys, Chennai and nSiC is purchased from Nanoshel, India Pvt. Ltd. The average size of nSiC considered is about 45-65 nm. Figure 1 presents the SEM micrographs of as received AZ31 alloy, nSiC and X-ray diffraction (XRD) of nSiC obtained.

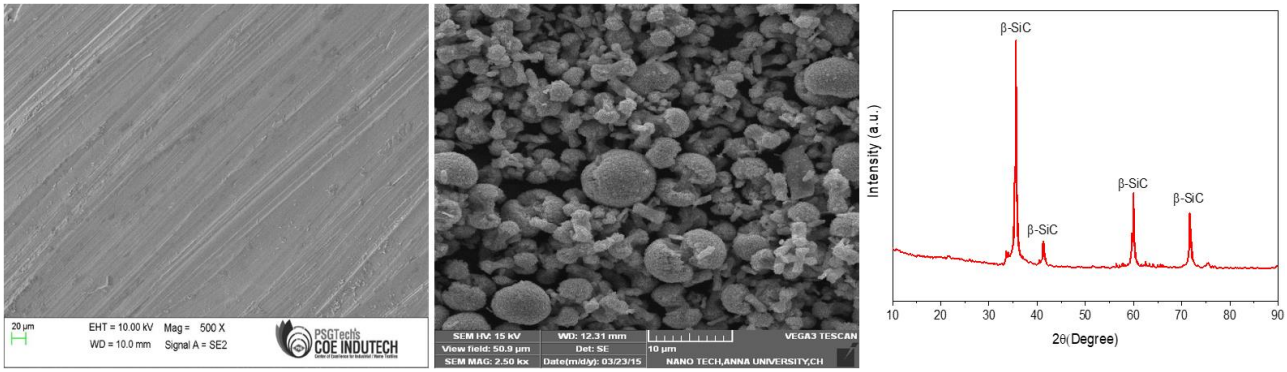

Figure 1. SEM micrograph of AZ31, nSiC and XRD of nSiC

For performing FSP, the CNC vertical machining center (VMC) is used with a cylindrical tool made from H13 alloy that is surface hardened to 55 HRC, including a 24 mm shoulder diameter, a 6x5 mm pin diameter, and length as shown in Figure 2 [21]. The VMC is YCM-EV 1020A with 45-1,000 rpm spindle speed, BT40 nose taper, and 5.5 kW motor is utilized. Initially, micro-sized drills were made on the surface of the AZ31 plate of size 100x100x10 mm for a depth of 4 mm. A pin-less tool was used to close the groove, and the holes were stuffed with nSiC according to the required weight proportion [22]. The next step is to execute the FSP at 500 rpm of rotation speed, 50 mm/min traverse speed, and 5 kN AL [23].

Figure 2. CNC machine, tool, and FSPed specimen

ASTM G99 is a widely recognized standard method used to conduct wear testing on a pin-on-disk (PoD) test apparatus. This method is commonly employed in academic and research settings to evaluate the materials' wear features. The quantification of wear is primarily influenced by various factors in the system, including the AL, such as material qualities, environmental factors, sliding speed, SD, and machine parameters [24]. For testing purposes, we will evaluate specimens made from the FSPed surface. These specimens consist of 9 mm diameter cylindrical pins with a length of 15 mm. We will also use a surface-hardened EN31 disc as the counterface material. [25]. Figure 3 shows the PoD apparatus with an attachment of a pin.

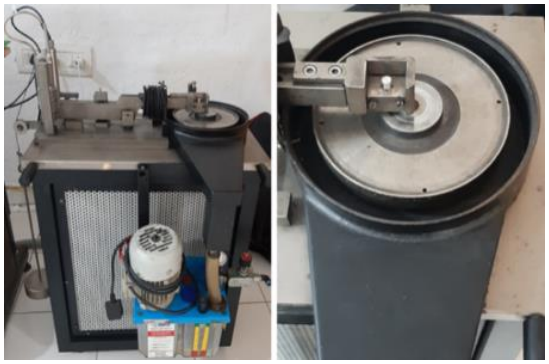

Figure 3. PoD apparatus and pin setup

3. Results and Discussion

With constant process parameters FSP is performed on the AZ31 substrate for incorporating nSiC to improve its properties. The performance of the AZ31 alloy as received and that of the surface-modified AZ31 alloy are examined. Figure 4 presents the scanning electron microscopic images of the as-received and FSPed samples with different nSiC content. Inferences show that material fusion occurs due to extreme heat produced due to the friction developed by the rotating tool on the sample surface [26]. Grain refinement occurs during solidification, which influences the mechanical strength and hardness of the surface composites. The fine grain refinement continues until the addition of 3 wt.% of nSiC, and higher addition leads to aggregation of nanoparticles to micron-sized particles that produce lower strength than their lower counterparts [27].

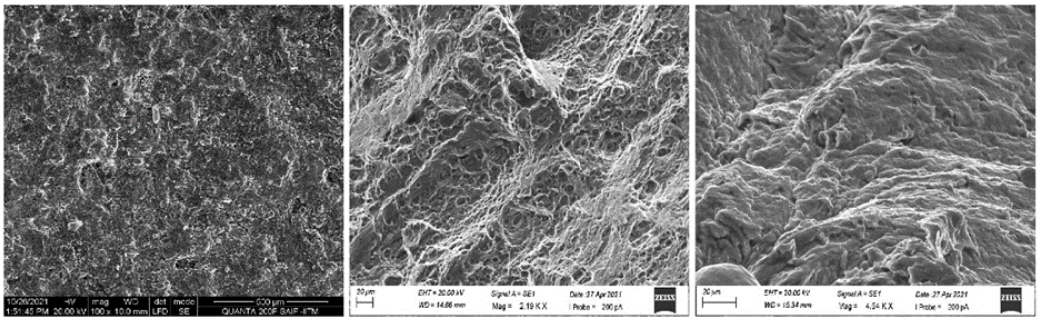

(a) As received AZ31 (b) AZ31+1%nSiC (c) AZ31+2%nSiC

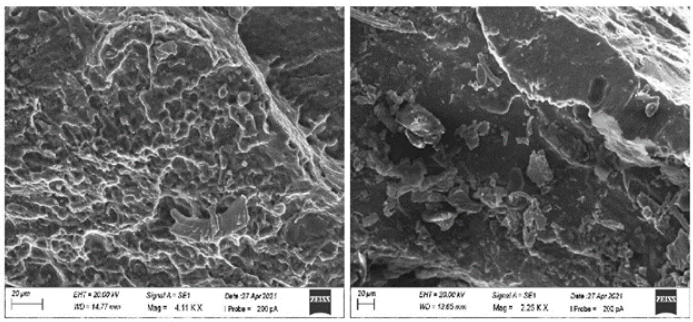

(d) AZ31+3%nSiC (e) AZ31+4%nSiC

Figure 4. SEM micrographs of specimens

The WR was calculated based on the wear loss method by measuring the volume before and after the fabricated FSPed samples were subjected to wear tests [28]. The DAQ system attached to PoD is used to capture the CoF. Irrespective of the nSiC inclusion on the surface of AZ31 alloy, the WR tends to rise with higher AL on the cylindrical pin, as presented in Figure 5. As the nSiC wt.% increases on the surface of AZ31, better strength and hardness is obtained, which resists deformation and wear. Lower WR is received till the inclusion of 3 wt.% of nSiC; adding more nSiC results in reduced strength and hardness due to nanoparticle aggregation, leading to higher WR [29, 30].

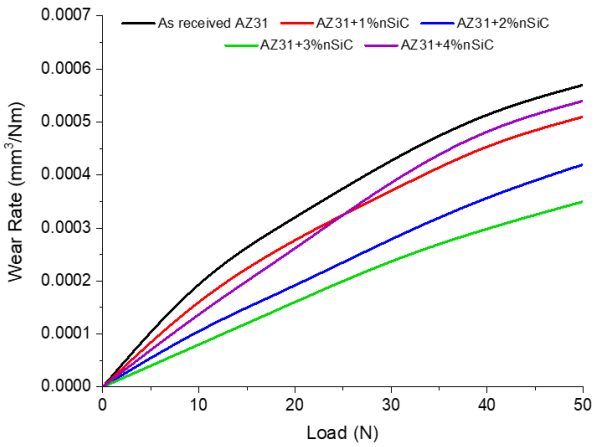

Figure 5. Impact of AL on WR

Figure 6 presents the change in WR for different conditions of SD. With an increase in SD there is a substantial increase in WR. Higher sliding velocities can soften the surface of an alloy or composite, which can decrease shear strength and increase WR. Increasing sliding speeds can cause changes in strain rate and friction heating, which can slightly increase WR over time [31]. Sliding over long distances can also harden the surface layer composition of waste debris, reducing wear; hence, a flattened curve is seen over higher values of SD [32]. When the amount of reinforcing particle material increased gradually, the WR was significantly reduced because high hard phases formed [33].

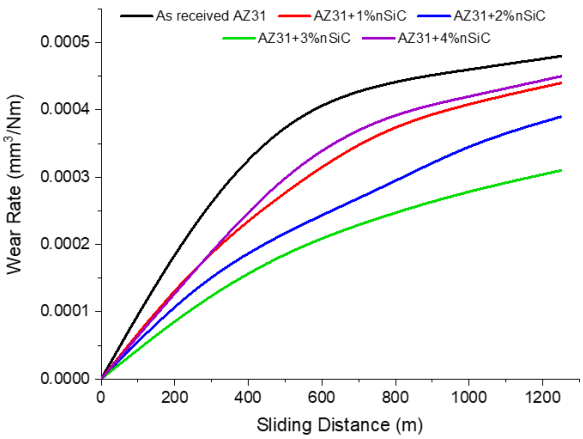

Figure 6. Impact of SD on WR

The CoF obtained during the wear test of AZ31-nSiC surface composite for various ALs is presented in Figure 7. As the load increases there is a substantial increase in CoF initially and then tends to lower, whereas higher inclusion of nSiC provides lower CoF. The CoF decreases with increasing normal load [34]. This is because greater loads and higher speeds cause a larger force-bearing area and smaller local stress, which reduces the CoF. A higher load causes more friction heat, softening the material and lowering the CoF [35].

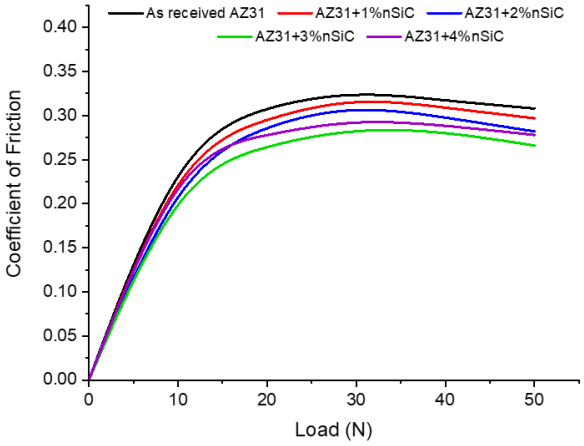

Figure 7. Influence of AL on CoF

The change in CoF for varying SD is shown in Figure 8. Higher inclusion of nSiC on AZ31 presents lower CoF due to the hardness imparted by the reinforcements on the surface. The test pin surface's thermal softening causes the CoF to drop as sliding velocity increases. The pin specimen experiences a decrease in hardness due to thermal softening, causing the CoF to fall [36]. However, a higher testing period can lead to more tribo-oxides, which can decrease WR and CoF. Pin substance and sliding counter disc adhere to one another; breaking their contact requires a larger frictional force, increasing CoF to be seen initially in all specimens [37].

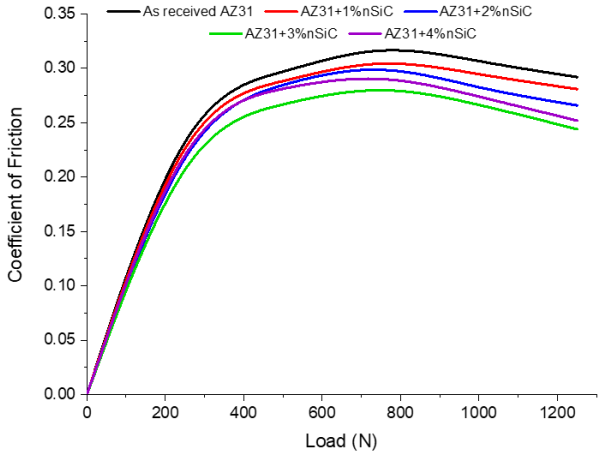

Figure 8. Influence of SD on CoF

Figure 9 and Figure 10 present the optical images of worn-out surfaces taken from each tested samples subjected to different loads and SD. The wear track is visible with higher wear debris on all the specimens. The 4 wt.% nSiC surface composite shows higher wear depth due to improper dispersal of nSiC and agglomeration. The nanoparticles serve to strengthen the matrix through mechanisms like load transfer, grain refinement, and the pinning of dislocations. During wear, the nanoparticles act as barriers that inhibit the direct contact between sliding surfaces, reducing adhesion and material loss. Additionally, these particles can form a protective tribolayer on the worn surface, which further minimizes wear by providing a low-friction interface. At high loads and SDs, the wear mechanisms that are seen are plastic deformation, delamination, and abrasion [38].

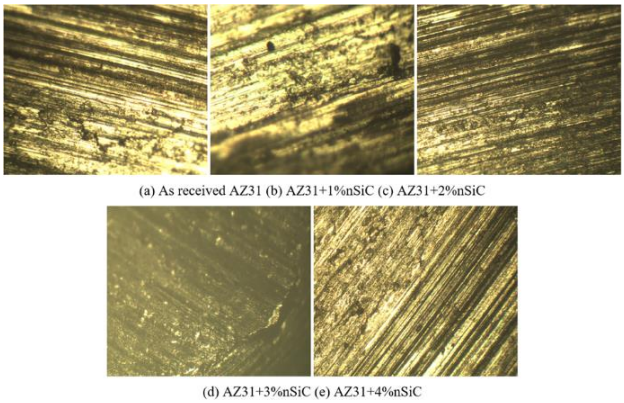

Figure 9. Worn surfaces of specimens subjected to varying AL

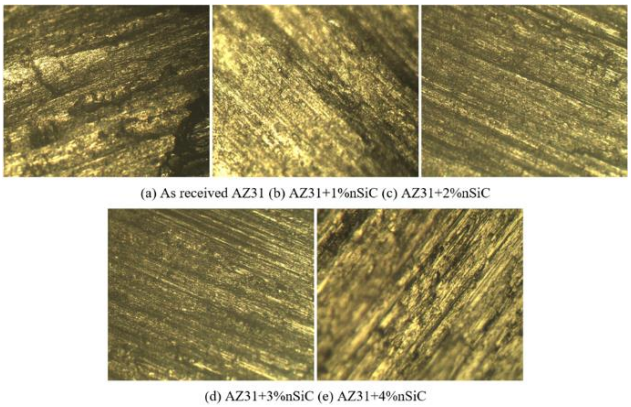

Figure 10. Worn surfaces of specimens subjected to varying SD

The plowing-type wear mechanism is also visualized in all the specimens. At higher loads and until moderate SDs, oxidation is also observed due to higher frictional heat developed at the interface of the pin surface and rotating disc counterface [39, 40]. During abrasive wear, hard particles scratch or plow the surface; in adhesive wear material transfer occurs between contacting surfaces; and in oxidative wear, a protective oxide layer is formed and subsequently worn away [41, 42].

4. Conclusion

The PoD wear tests are adopted to investigate the wear performance of FSPed AZ31-nSiC surface composites subjected to various ALs and SDs. Observation shows that;

- Microscopic images revealed grain refinement during solidification, which influences the mechanical strength and hardness of the surface composites. The fine grain refinement continues until 3 wt.% of nSiC is added, and higher addition leads to agglomeration of nanoparticles to micron-sized particles that produce lower strength than their lower counterparts.
- The WR is lower till the inclusion of 3 wt.% of nSiC; adding more nSiC results in reduced strength and hardness due to nanoparticle accumulation, leading to higher WR. With an increase in SD there is a substantial increase in WR. Higher sliding velocities can soften the surface of an alloy or composite, which can

decrease shear strength and increase WR. The creation of high hard phases led to a progressive rise in the amount of reinforcing particle content, significantly reducing the WR.

- With higher ALs, there is a substantial increase in CoF initially and then tends to lower, whereas higher inclusion of nSiC provides lower CoF. A higher load causes more friction heat, softening the material and reducing the CoF. Higher inclusion of nSiC on AZ31 presents lower CoF due to the hardness imparted by the reinforcements on the surface. The test pin surface's thermal softening causes the CoF to drop as sliding velocity increases. The pin specimen's hardness decreases due to this thermal softening, which lowers CoF.
- The optical images show clear wear tracks with higher wear debris, 4 wt.% nSiC surface composite shows higher wear depth due to poor dispersal of nSiC and agglomeration. Various wear mechanisms are abrasion, delamination, and plastic deformation.
- As compared with an AL of 10 N, the AL of 50 N produces a 171.43% higher WR for as received alloy, for AZ31+3%nSiC, the WL is increased by 337.5% whereas the CoF is increased by 14.93% for as received alloy and 15.15% for AZ31+3%nSiC composite. Similarly, increasing the SD from 250 to 1250m, the WR is doubled for as received alloy and 181.82% for AZ31+3%nSiC, the CoF is increased by 0.41%.

Funding

This research received no external funding

Author contributions

N. Senthilkumar: Conceptualization, Methodology, Writing-Original draft preparation, Software, Validation. **B. Deepanraj:** Experimentation, Visualization, Investigation, Writing and Editing. **Feroz Shaik:** Supervision, Validation, Review and Editing. **V. Nadanakumar:** Conceptualization, Methodology, Review and Editing.

Conflicts of interest

The authors declare no conflicts of interest.

References

1. Dong, H. (2010). Surface Engineering of Light Alloys: Aluminium, Magnesium and Titanium Alloys. Elsevier Science. https://books.google.co.in/books?id=wAPfQwAACAAJ
2. Omarov, S., Nauryz, N., Talamona, D., & Perveen, A. (2022). Surface Modification Techniques for Metallic Biomedical Alloys: A Concise Review. Metals, 13(1), 82. https://doi.org/10.3390/met13010082
3. Gezer, U., Demir, B., Kepir, Y., Gunoz, A., & Kara, M. (2023). A numerical study on the low-velocity impact response of hybrid composite materials. Turkish Journal of Engineering, 7(4), 314–321. https://doi.org/10.31127/tuje.1191785
4. Cagan, S. C. ., & Buldum, B. B. . (2021). Influence of the effect of the ball burnishing process applied to Al 7075-T6 alloy in different nano-aluminum powder-added grease environment on surface quality. Advanced Engineering Science, 1, 20–25.
5. Davis, R., Singh, A., Debnath, K., Keshri, A. K., Soares, P., Sopchenski, L., Terryn, H. A., & Prakash, V. (2023). Surface modification of biodegradable Mg alloy by adapting μEDM capabilities with cryogenically-treated tool electrodes. The International Journal of Advanced Manufacturing Technology, 126(9–10), 4617–4636. https://doi.org/10.1007/s00170-023-11395-0
6. Mahto, V. K., Singh, A. K., & Malik, A. (2023). Surface modification techniques of magnesium-based alloys for implant applications. Journal of Coatings Technology and Research, 20(2), 433–455. https://doi.org/10.1007/s11998-022-00716-9
7. Akinlabi, E. T., & Mahamood, R. M. (2020). Solid-State Welding: Friction and Friction Stir Welding Processes. Springer International Publishing. https://books.google.co.in/books?id=rdfIDwAAQBAJ
8. Gupta, M. K. (2020). Friction stir process: a green fabrication technique for surface composites—a review paper. SN Applied Sciences, 2(4), 532. https://doi.org/10.1007/s42452-020-2330-2
9. Subramani, M., Huang, S.-J., & Borodianskiy, K. (2022). Effect of SiC Nanoparticles on AZ31 Magnesium Alloy. Materials, 15(3), 1004. https://doi.org/10.3390/ma15031004
10. Shen, M., Zhu, X., Han, B., Ying, T., & Jia, J. (2022). Dry sliding wear behaviour of AZ31 magnesium alloy strengthened by nanoscale SiCp. Journal of Materials Research and Technology, 16, 814–823. https://doi.org/10.1016/j.jmrt.2021.12.048
11. Padmavathi, K. R., Alharbi, S. A., Venkatesh, R., & Sivaprakash, E. (2024). SiC Blending Behaviour of Hybrid AZ31 Alloy Nanocomposite: Metallographic and Mechanical Studies. Silicon. 16, 2771–2779, https://doi.org/10.1007/s12633-024-02880-6
12. Abdollahzadeh, A., Shokuhfar, A., Omidvar, H., Cabrera, J., Solonin, A., Ostovari, A., & Abbasi, M. (2019). Structural evaluation and mechanical properties of AZ31/SiC nano-composite produced by friction stir welding process at various welding speeds. Proceedings of the Institution of Mechanical Engineers, Part L: Journal of Materials: Design and Applications, 233(5), 831–841. https://doi.org/10.1177/1464420717708485
13. Kumar, T. S., Raghu, R., Thankachan, T., Čep, R., & Kalita, K. (2024). Mechanical property analysis and dry sand three-body abrasive wear behaviour of AZ31/ZrO2 composites produced by stir casting. Scientific Reports, 14(1), 1543. https://doi.org/10.1038/s41598-024-52100-9
14. Kumar, T. S., Thankachan, T., Shalini, S., Čep, R., & Kalita, K. (2023). Microstructure, hardness and

wear behavior of ZrC particle reinforced AZ31 surface composites synthesized via friction stir processing. Scientific Reports, 13(1), 20089. https://doi.org/10.1038/s41598-023-47381-5

15. Xiong, G. Y., Yu, M., & Zhao, L. Z. (2012). AZ31 Magnesium Alloy Surface Laser Alloying of SiC-316L Composite Coating. Advanced Materials Research, 538–541, 243–246. https://doi.org/10.4028/www.scientific.net/AMR.538-541.243
16. Jiang, H. Y., Ding, W. Bin, Zeng, X. Q., Li, D. H., & Yao, S. S. (2007). Mechanical Behavior of Gas Tungsten Arc Surface Modified Composite Layer on Mg Alloy AZ31 with SiC p and Aluminum. Materials Science Forum, 546–549, 485–490. https://doi.org/10.4028/www.scientific.net/MSF.546-549.485
17. Arora, H. S., Singh, H., Dhindaw, B. K., & Grewal, H. S. (2012). Improving the Tribological Properties of Mg Based AZ31 Alloy Using Friction Stir Processing. Advanced Materials Research, 585, 579–583. https://doi.org/10.4028/www.scientific.net/AMR.585.579
18. Dziubińska, A., Gontarz, A., Horzelska, K., & Pieśko, P. (2015). The Microstructure and Mechanical Properties of AZ31 Magnesium Alloy Aircraft Brackets Produced by a New Forging Technology. Procedia Manufacturing, 2, 337–341. https://doi.org/10.1016/j.promfg.2015.07.059
19. Li, X., Zhang, M., Fang, X., Li, Z., Jiao, G., & Huang, K. (2023). Improved strength-ductility synergy of directed energy deposited AZ31 magnesium alloy with cryogenic cooling mode. Virtual and Physical Prototyping, 18(1), e2170252. https://doi.org/10.1080/17452759.2023.2170252
20. Gizowska, M., Piątek, M., Perkowski, K., & Antosik, A. (2023). Influence of Sintering Conditions and Nanosilicon Carbide Concentration on the Mechanical and Thermal Properties of Si3N4-Based Materials. Materials, 16(5), 2079. https://doi.org/10.3390/ma16052079
21. Abd Elnabi, M. M., El Mokadem, A., & Osman, T. (2022). Optimization of process parameters for friction stir welding of dissimilar aluminum alloys using different Taguchi arrays. The International Journal of Advanced Manufacturing Technology, 121(5–6), 3935–3964. https://doi.org/10.1007/s00170-022-09531-3
22. Manroo, S. A., Khan, N. Z., & Ahmad, B. (2022). Study on surface modification and fabrication of surface composites of magnesium alloys by friction stir processing: a review. Journal of Engineering and Applied Science, 69(1), 25. https://doi.org/10.1186/s44147-022-00073-9
23. Kumar, A., Singh, V. P., Nirala, A., Singh, R. C., Chaudhary, R., Mourad, A.-H. I., Sahoo, B. K., & Kumar, D. (2023). Influence of tool rotational speed on mechanical and corrosion behaviour of friction stir processed AZ31/Al2O3 nanocomposite. Journal of Magnesium and Alloys, 11(7), 2585–2599. https://doi.org/10.1016/j.jma.2023.06.012
24. Muralidhara, B., Babu, S. K., & Suresha, B. (2020). Studies on mechanical, thermal and tribological properties of carbon fibre-reinforced boron nitride-filled epoxy composites. High Performance Polymers, 32(9), 1061–1081. https://doi.org/10.1177/0954008320929396
25. Vasanthkumar, P., Balasundaram, R., & Senthilkumar, N. (2022). Sliding-friction wear of a seashell particulate reinforced polymer matrix composite: modeling and optimization through RSM and Grey Wolf optimizer. Transactions of the Canadian Society for Mechanical Engineering, 46(2), 329–345. https://doi.org/10.1139/tcsme-2021-0139
26. Bhojan, A., Senthilkumar, N., & Deepanraj, B. (2016). Parametric Influence of Friction Stir Welding on Cast Al6061/20%SiC/2%MoS_2 MMC Mechanical Properties. Applied Mechanics and Materials, 852, 297–303. https://doi.org/10.4028/www.scientific.net/AMM.852.297
27. Wang, R., Xiong, Y., Yang, K., Zhang, T., Zhang, F., Xiong, B., Hao, Y., Zhang, H., Chen, Y., & Tang, J. (2023). Advanced progress on the significant influences of multi-dimensional nanofillers on the tribological performance of coatings. RSC Advances, 13(29), 19981–20022. https://doi.org/10.1039/D3RA01550E
28. Radhika, N., Krishna, S. A., Basak, A. K., & Adediran, A. A. (2024). Microstructure and tribological behaviour of CoCrCuFeTi high entropy alloy reinforced SS304 through friction stir processing. Scientific Reports, 14(1), 3662. https://doi.org/10.1038/s41598-024-54267-7
29. Ostovan, F., Azimifar, I., Toozandehjani, M., Shafiei, E., & Shamshirsaz, M. (2021). Synthesis of ex-situ Al5083 reinforced with mechanically-alloyed CNTs and Fe2O3 nanoparticles using friction stir processing. Journal of Materials Research and Technology, 14, 1670–1681. https://doi.org/10.1016/j.jmrt.2021.07.072
30. Durowaye, S., Sekunowo, O., Bolasodun, B., Oduaran, İ., & Lawal, G. (2019). Mechanical and wear characterisation of quarray tailing reinforced A6063 metal matrix composites. Turkish Journal of Engineering, 3(3), 133–139. https://doi.org/10.31127/tuje.490509
31. Sundara Selvan, S., & Senthilkumar, N. (2018). Dry sliding wear behaviour of surface modified az61 magnesium alloy reinforced with nano titanium dioxide. Journal of the Balkan Tribological Association, 24(3), 429–452.
32. Suresh, R. (2020). Comparative study on dry sliding wear behavior of mono (Al2219/B 4 C) and hybrid (Al2219/B 4 C/Gr) metal matrix composites using statistical technique. Journal of the Mechanical Behavior of Materials, 29(1), 57–68. https://doi.org/10.1515/jmbm-2020-0006
33. Vithal, N. D., Krishna, B. B., & Krishna, M. G. (2021). Impact of dry sliding wear parameters on the wear rate of A7075 based composites reinforced with ZrB2 particulates. Journal of Materials Research and Technology, 14, 174–185. https://doi.org/10.1016/j.jmrt.2021.06.005

34. Sundaraselvan, S., Senthilkumar, N., Tamizharasan, T., & Sait, A. N. (2020). Surface modification of AZ61 Magnesium Alloy with Nano TiO2/Al2O3 using Laser Cladding Technique. Materials Today: Proceedings, 21, 717–721. https://doi.org/10.1016/j.matpr.2019.06.745
35. Liu, C. T., Chang, Y. P., & Yeh, J. W. (2022). Study on friction properties of different abrasive materials and polylactic acid materials. Journal of Physics: Conference Series, 2345(1), 012027. https://doi.org/10.1088/1742-6596/2345/1/012027
36. Subramanian, K., Murugesan, S., Mohan, D. G., & Tomków, J. (2021). Study on Dry Sliding Wear and Friction Behaviour of Al7068/Si3N4/BN Hybrid Composites. Materials, 14(21), 6560. https://doi.org/10.3390/ma14216560
37. Suganeswaran, K., Parameshwaran, R., Mohanraj, T., & Radhika, N. (2021). Influence of secondary phase particles Al 2 O 3 /SiC on the microstructure and tribological characteristics of AA7075-based surface hybrid composites tailored using friction stir processing. Proceedings of the Institution of Mechanical Engineers, Part C: Journal of Mechanical Engineering Science, 235(1), 161–178. https://doi.org/10.1177/0954406220932939
38. Bhandari, R., Biswas, P., Mallik, M., & Mondal, M. K. (2024). Dry and Lubrication Sliding Wear Characteristics and Wear Mechanism Mapping for In Situ Al–25Mg 2 Si Composites. Advanced Engineering Materials, 26(2), 2300845https://doi.org/10.1002/adem.202300845
39. Gunoz, A., Kepir, Y., & Kara, M. (2022). The investigation of hardness and density properties of GFRP composite pipes under seawater conditions. Turkish Journal of Engineering, 6(1), 34–39. https://doi.org/10.31127/tuje.775536
40. Srivyas, P. D., & Charoo, M. S. (2020). Tribological behavior of aluminum silicon eutectic alloy-based composites under dry and wet sliding for variable load and sliding distance. SN Applied Sciences, 2(10), 1654. https://doi.org/10.1007/s42452-020-03433-3
41. Sabari, K., Muniappan, A., & Singh, M. (2024). Enhancing Microstructural Characteristics and Mechanical Properties in Friction Stir Welding of Thick Magnesium Alloy Plates through Optimization. SAE Technical Paper, 2024-01-5014 https://doi.org/10.4271/2024-01-5014
42. Sathish, T., Kaladgi, A. R. R., Mohanavel, V., Arul, K., Afzal, A., Aabid, A., Baig, M., & Saleh, B. (2021). Experimental Investigation of the Friction Stir Weldability of AA8006 with Zirconia Particle Reinforcement and Optimized Process Parameters. Materials, 14(11), 2782. https://doi.org/10.3390/ma14112782